Title

Splice-site mutations identified in PDE6A responsible for retinitis pigmentosa in consanguineous Pakistani families.

Authors

Khan, Shahid Y
Ali, Shahbaz
Naeem, Muhammad Asif
et al.

Publication Date

2015

Peer reviewed

Molecular Vision 2015; 21:871-882 <http://www.molvis.org/molvis/v21/871>
Received 1 July 2014 | Accepted 15 August 2015 | Published 18 August 2015

Splice-site mutations identified in *PDE6A* responsible for retinitis pigmentosa in consanguineous Pakistani families

Shahid Y. Khan,[1] Shahbaz Ali,[2] Muhammad Asif Naeem,[2] Shaheen N. Khan,[2] Tayyab Husnain,[2] Nadeem H. Butt,[3] Zaheeruddin A. Qazi,[4] Javed Akram,[3,5] Sheikh Riazuddin,[2,3,5] Radha Ayyagari,[6] J. Fielding Hejtmancik,[7] S. Amer Riazuddin[1]

(The first two and last two authors contributed equally to this work.)

[1]The Wilmer Eye Institute, Johns Hopkins University School of Medicine, Baltimore MD; [2]National Centre of Excellence in Molecular Biology, University of the Punjab, Lahore, Pakistan; [3]Allama Iqbal Medical College, University of Health Sciences, Lahore, Pakistan; [4]Layton Rahmatulla Benevolent Trust Hospital, Lahore Pakistan; [5]National Centre for Genetic Diseases, Shaheed Zulfiqar Ali Bhutto Medical University, Islamabad Pakistan; [6]Shiley Eye Institute, University of California San Diego, La Jolla CA; [7]Ophthalmic Genetics and Visual Function Branch, National Eye Institute, National Institutes of Health, Bethesda MD

Purpose: This study was conducted to localize and identify causal mutations associated with autosomal recessive retinitis pigmentosa (RP) in consanguineous familial cases of Pakistani origin.
Methods: Ophthalmic examinations that included funduscopy and electroretinography (ERG) were performed to confirm the affectation status. Blood samples were collected from all participating individuals, and genomic DNA was extracted. A genome-wide scan was performed, and two-point logarithm of odds (LOD) scores were calculated. Sanger sequencing was performed to identify the causative variants. Subsequently, we performed whole exome sequencing to rule out the possibility of a second causal variant within the linkage interval. Sequence conservation was performed with alignment analyses of *PDE6A* orthologs, and in silico splicing analysis was completed with Human Splicing Finder version 2.4.1.
Results: A large multigenerational consanguineous family diagnosed with early-onset RP was ascertained. An ophthalmic clinical examination consisting of fundus photography and electroretinography confirmed the diagnosis of RP. A genome-wide scan was performed, and suggestive two-point LOD scores were observed with markers on chromosome 5q. Haplotype analyses identified the region; however, the region did not segregate with the disease phenotype in the family. Subsequently, we performed a second genome-wide scan that excluded the entire genome except the chromosome 5q region harboring *PDE6A*. Next-generation whole exome sequencing identified a splice acceptor site mutation in intron 16: c.2028–1G>A, which was completely conserved in *PDE6A* orthologs and was absent in ethnically matched 350 control chromosomes, the 1000 Genomes database, and the NHLBI Exome Sequencing Project. Subsequently, we investigated our entire cohort of RP familial cases and identified a second family who harbored a splice acceptor site mutation in intron 10: c.1408–2A>G. In silico analysis suggested that these mutations will result in the elimination of wild-type splice acceptor sites that would result in either skipping of the respective exon or the creation of a new cryptic splice acceptor site; both possibilities would result in retinal photoreceptor cells that lack PDE6A wild-type protein.
Conclusions: we report two splice acceptor site variations in *PDE6A* in consanguineous Pakistani families who manifested cardinal symptoms of RP. Taken together with our previously published work, our data suggest that mutations in *PDE6A* account for about 2% of the total genetic load of RP in our cohort and possibly in the Pakistani population as well.

The term retinitis pigmentosa (RP) refers to bone spicule-like pigmentation in the mid-peripheral fundus that stimulates inflammation and was first used by the German physician Donders in 1857 [1]. RP is a progressive rod-cone dystrophy that primarily affects the rod photoreceptors whereas the function of the cone receptors is compromised as the disease progresses [2]. Ocular findings comprise atrophic changes in the photoreceptors and in the retinal pigment epithelium (RPE) followed by the appearance of melanin-containing structures in the retinal vascular layer [2]. The typical fundus appearance includes attenuated arterioles, bone spicule-like pigmentation, and waxy pallor of the optic disc. Affected individuals often have severely abnormal or non-detectable rod responses in electroretinogram (ERG) recordings even in the early stage of the disease [2].

RP is the most common inherited retinal dystrophy, affecting approximately 1 in 5,000 individuals worldwide [3]. RP is clinically and genetically heterogeneous, which is inherited as a dominant, recessive, as well as an X-linked trait [4]. RP presents intra- and interfamilial variations in expressivity, penetrance, progression, and age of onset [5]. Among the several causes of variable phenotypes are alternative

Correspondence to: S. Amer Riazuddin, The Wilmer Eye Institute, Johns Hopkins University School of Medicine, 600 N. Wolfe Street, Maumenee 840, Baltimore, MD 21287; Phone: (410) 955-3656; FAX: (410) 955-3656; email: riazuddin@jhmi.edu

alleles, environmental factors, modifier genes, or a combination of these factors [6,7]. Autosomal recessive RP (arRP) is the most common form of RP worldwide, and to date, 36 genes/loci have been associated with autosomal recessive RP (RetNet).

Phosphodiesterase 6 (PDE6) is a critical enzyme of the visual phototransduction cascade in the vertebrate retina [8,9]. The protein is a heterotrimer that consists of an alpha, a beta, and two gamma subunits. *PDE6A* (Gene ID: 5145; OMIM: 180071) encodes for the α-subunit of cyclic guanosine monophosphate (cGMP)-phosphodiesterase that is primarily expressed in rod photoreceptors [10,11]. *PDE6A* consists of 22 coding exons and encodes for 860 amino acids [12,13]. Dryja and colleagues were the first to report causal mutations in *PDE6A* in patients with arRP [14].

We previously reported three mutations in *PDE6A* including a splice acceptor site mutation in three families of Pakistani origin [15]. Here, we report two additional familial cases with multiple members manifesting symptoms of RP. The clinical phenotype was established with fundus photography and electroretinography while genome-wide linkage analyses localized the disease interval to chromosome 5q. Subsequently, Sanger sequencing identified splice acceptor site mutations in these two families that were absent in ethnically matched control chromosomes.

METHODS

Clinical ascertainment: A total of >300 consanguineous Pakistani families with non-syndromic retinal dystrophies were recruited to identify new disease loci responsible for inherited visual diseases. The institutional review boards (IRBs) of the National Centre of Excellence in Molecular Biology (Lahore, Pakistan), National Eye Institute (Bethesda, MD), and Johns Hopkins University (Baltimore, MD) approved the study. All participating family members provided informed written consent that has been endorsed by the respective IRBs and is consistent with the tenets of the Declaration of Helsinki.

A detailed clinical and medical history was obtained from the individual families. Funduscopy was performed at Layton Rehmatulla Benevolent Trust (LRBT) Hospital (Lahore, Pakistan). ERG measurements were recorded by using equipment manufactured by LKC (Gaithersburg, MD). Dark-adapted rod responses were determined through incident flash attenuated with −25 dB, whereas the rod–cone responses were measured at 0 dB. The 30 Hz flicker responses were recorded at 0 dB to a background illumination of 17 to 34 cd/m^2.

All participating members voluntarily provided approximately 10 ml of blood sample that was stored in 50 ml Sterilin® falcon tubes containing 400 µl of 0.5 M EDTA. Blood samples were stored at −20 °C for long-term storage.

Genomic DNA extraction: Genomic DNA was extracted from white blood cells using a non-organic modified procedure as described previously [16,17]. Approximately, 10 ml blood samples were mixed with 35 ml of TE buffer (10 mM Tris-HCl, 2 mM EDTA, pH 8.0) and the TE-blood mixture was centrifuged at 2,000 x g for 20 min. The red blood cells were discarded and the pellet was re-suspended in 35 ml of TE buffer. The TE washing was repeated for 2–3 times and the washed pellet was re-suspended in 2 ml of TE buffer. Next, 6.25 ml of protein digestion cocktail (50 µl [10 mg/ml] of proteinase K, 6 ml TNE buffer [10 mM Tris HCl, 2 mM EDTA, 400 mM NaCl] and 200 µl of 10% sodium dodecyl sulfate) was added to the re-suspended pellets and incubated overnight in a shaker (250 rpm) at 37 °C. The digested proteins were precipitated by adding 1 ml of 5 M NaCl, followed by vigorous shaking and chilling on ice for 15 min. The precipitated proteins were pelleted by centrifugation at 2,000 x g for 20 min and removed. The supernatant was mixed with equal volumes of phenol/chloroform/isoamyl alcohol (25:24:1) and the aqueous layer containing the genomic DNA was carefully collected. The DNA was precipitated with isopropanol and pelleted by centrifugation at 3,500 x g for 15 min. The DNA pellets were washed with 70% ethanol and dissolved in TE buffer. The concentration of the extracted genomic DNA was estimated with a SmartSpec plus Bio-Rad Spectrophotometer (Bio-Rad, Hercules, CA).

Genotype analysis: Applied Biosystems MD-10 linkage mapping panels (Foster City, CA) were used to complete the genome-wide scan for family PKRP133. Multiplex PCR was completed as described previously [15]. The PCR products were mixed with a loading cocktail that contained HD-400 size standards (Applied Biosystems) and were resolved in an Applied Biosystems 3100 DNA Analyzer. Genotypes were assigned using the GeneMapper software from Applied Biosystems. Exclusion analyses were completed for PKRP140 using closely spaced short tandem repeat (STR) markers. The sequence of the primer pairs used for the exclusion analyses and amplification conditions are available upon request.

Linkage analysis: Linkage analysis was performed with the alleles of PKRP133 obtained through the genome-wide scan and the alleles of PKRP140 obtained through exclusion analysis using the FASTLINK version of MLINK from the LINKAGE Program Package [18,19]. Maximum logarithm of odds (LOD) scores were calculated using ILINK from the LINKAGE Program Package. arRP was investigated as a

fully penetrant disorder that has an affected allele frequency of 0.001.

Mutation screening: Primer pairs to amplify the coding exons along with exon-intron boundaries of *PDE6A* were designed using primer3 program and are available upon request. PCR amplification consisted of a denaturation step at 95 °C for 5 min followed by a two-step touchdown procedure. The first step of 10 cycles consisted of denaturation at 95 °C for 30 s, followed by primer set specific (available upon request) annealing for 30 s (annealing temperature decrease by 1 °C per cycle) and elongation at 72 °C for 45 s. The second step of 30 cycles consisted of denaturation at 95 °C for 30 s followed by annealing (annealing 10 °C below the primer set specific annealing temperature) for 30 s and elongation at 72 °C for 45 s, followed by final elongation at 72 °C for 5 min.

The PCR primers for each exon were used for bidirectional sequencing using the BigDye Terminator Ready reaction mix according to the manufacturer's instructions. The sequencing products were resolved on an ABI PRISM 3100 DNA analyzer (Applied Biosystems), and the results were analyzed with Applied Biosystems SeqScape software.

Exome sequencing and variant identification: Exome capture library preparation, next-generation sequencing, and variant calling were completed commercially at the Cincinnati Children's Hospital and Medical Center (CCHMC) core facility. Genomic DNA was captured with the Agilent SureSelect Human All Exon kit according to the manufacturer's instructions (Agilent, Palo Alto, CA). After capture and enrichment, the whole exome paired-end library was sequenced on the Illumina HiSeq 2000 Genome Analyzer (Illumina Inc., San Diego, CA). Approximately 75% of the reads were aligned to the reference sequence and passed quality-control filters, which was sufficient to generate on average 30X coverage for the exome.

The raw data was mapped to the University of California, Santa Cruz (UCSC) hg19 reference genome by ELAND; SNP and INDEL (insertion/deletion) calls were made according to the genome analysis toolkit (GATK) in exome sequencing and variant identification section. The whole exome data consisted on average of nearly 27,000 single-base changes. First, we removed all variants that were not present in the linkage interval. Then, we removed all alleles that were heterozygous for the reference allele in the affected individual. Finally, we excluded all single nucleotide polymorphisms (SNPs) with a minor-allele frequency (MAF) >2% in the affected individual.

In silico analysis: The degree of evolutionary conservation of positions at which mutations exist in other *PDE6A* orthologs was examined using the UCSC Genome browser. The effect of the c.1408–2A>G and c.2028–1G>A mutations on the *PDE6A* mRNA splicing was predicted with an online bioinformatics tool, the Human Splicing Finder 2.4.1 (HSF).

RESULTS

PKRP133 was recruited from the Punjab province of Pakistan. A total of 23 individuals including five affected individuals were enrolled in the study (Figure 1). Medical records and clinical reports of earlier examinations by the family physician suggested retinal dystrophy with early most likely congenital onset. Interviews with family elders revealed the initial presenting symptoms of night blindness and decreased visual acuity experienced by affected individuals in early childhood. We performed a detailed ophthalmic examination of selected individuals. Visual acuity in affected individuals 21 and 30 was limited, progressing to only counting fingers in affected individual 21 (Table 1). The fundus examination of affected individual 21 shows severe bone spicule-like pigmentation in the mid-periphery and periphery of the retina along with milder macular involvement, arteriolar attenuation, and disc pallor (Figure 2A). The fundus examination of affected individual 30 shows only milder macular involvement, arteriolar attenuation, and disc pallor, and no bone spicule-like pigmentation was observed in the mid-periphery and periphery of the retina (Figure 2B). The affected individuals had reduced ERG responses with delayed implicit time (Figure 3A–D). Photophobia or nystagmus was not observed in any affected or unaffected family member.

Initially, a genome-wide scan with 382 STR markers with an average spacing of approximately 10 cM was performed to localize the RP phenotype in PKRP133. Suggestive linkage with alleles of microsatellite markers on chromosome 5q, D5S422 and D5S400, was observed with LOD scores of 2.67 and 2.24 at θ=0.05, respectively. Haplotype analysis identified a region distal to D5S636 based upon recombination in affected individual 17 excluding *PDE6A* that lies approximately 5 Mb proximal of D5S636. The causal haplotype in the critical interval was segregated with the disease phenotype within the family with the exception of individual 33 (age: 24 years), who was homozygous for the disease haplotype (Figure 1). This individual was clinically evaluated over a period of 2 years, but no RP-like symptoms were observed. As shown in Figure 2, the fundus is normal with healthy retinal vasculature and the absence of any pigmentation in the peripheral and mid-peripheral regions of the retina (Figure 2C-D). Similarly, ERG recordings show normal ranges of the a- and b-waves with normal implicit time (Figure 3E-H). Taken together, the clinical evaluations of individual 33 over the course of the study (Figure 2C–D and Figure 3E-H)

confirmed that this individual is clinically unaffected and does not exhibit any symptoms of RP.

In view of the clinical and haplotype analyses of individual 33, an additional genome-wide linkage analysis was completed to rule out the possibility of additional evidence of linkage to a causal locus other than 5q33–35. Subsequently, a set of 399 additional markers were genotyped from the Linkage mapping set v.2.5-HD5, and taken together, all these markers refined the genome-wide resolution to approximately 5 cM spacing across the entire genome. A two-point LOD score of 2.84 at θ=0 was obtained with marker D5S2066 located distal to D5S422. Two-point LOD scores greater than 0.50 were also obtained for markers D3S3715, D5S471, D5S2115, D8S1771, D8S1820, D10S189, D13S173, D15S1002, D15S117, D16S3068, D16S503, D20S906, and D22S423. Linkage to all these markers was excluded either by large negative LOD scores calculated for closely flanking markers or by haplotype analysis.

Lack of identification of any potential locus other than on chromosome 5q during two separate genome-wide linkage scans and multiple clinical examinations of unaffected individual 33 that confirmed the absence of the clinical symptoms of RP prompted us to consider the following scenarios. First, affected individual 17 had been diagnosed

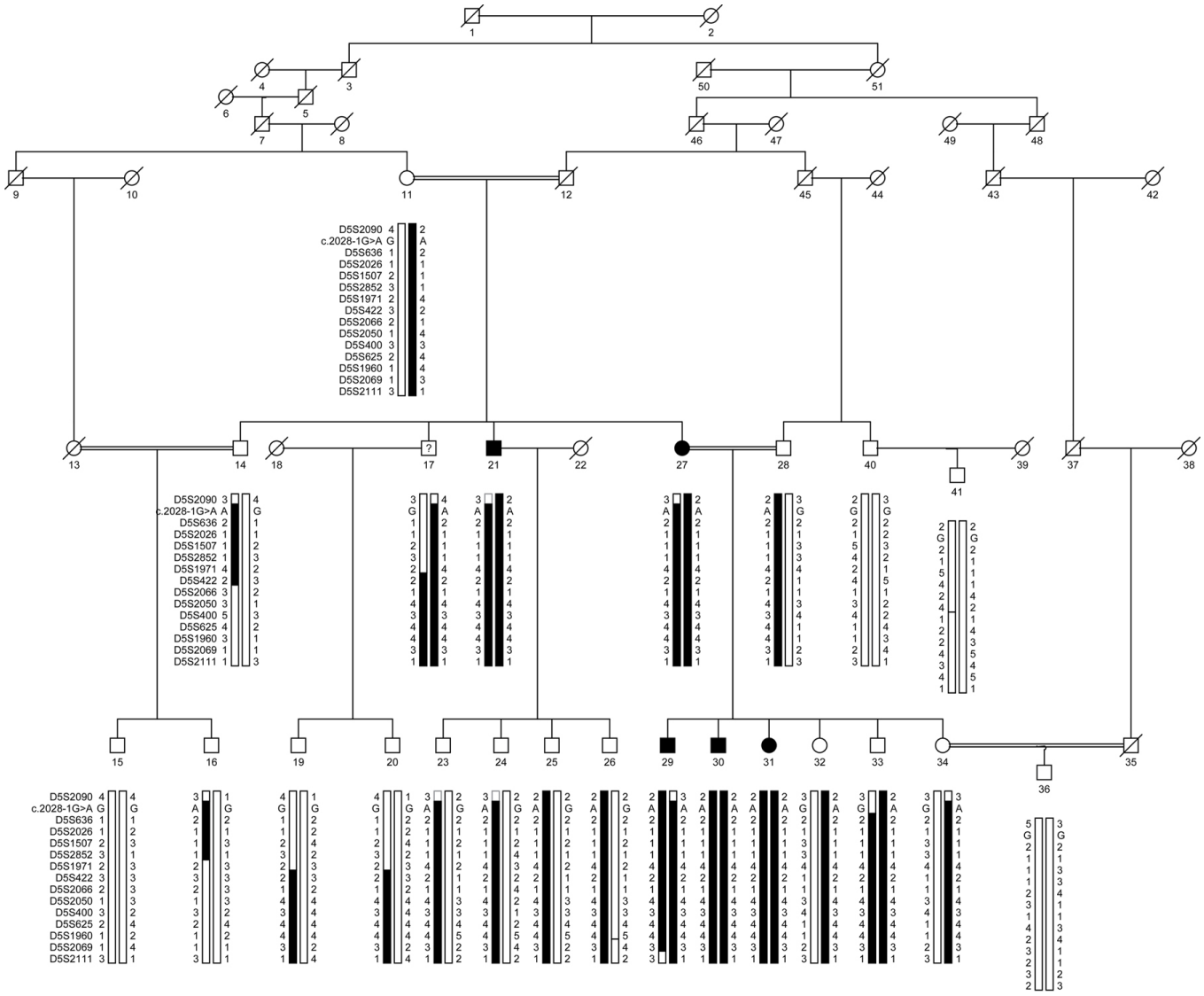

Figure 1. Pedigree of family PKRP133. Squares are males, circles are females, filled symbols are affected individuals, the double line between individuals indicates consanguinity, and the diagonal line through a symbol is a deceased family member. The haplotypes of 14 adjacent chromosome 5q33 microsatellite markers are shown. The alleles that form the risk haplotype are shaded black and the alleles that do not cosegregate with RP are shown in white.

incorrectly by the local ophthalmologist, and/or perhaps he manifested another form of retinal degeneration that had been misdiagnosed as RP. Second, affected individual 17 was a "phenocopy" manifesting the clinical phenotype of RP due to a genetic mutation not present on chromosome 5q. Initially, individual 17 voluntarily provided a blood sample; however, he has been reluctant to travel to an ophthalmology clinic for a thorough ocular examination. We approached affected individual 17 several times during the study and requested his cooperation for a comprehensive ocular examination without any success. Since we do not have conclusive evidence of the clinical phenotype, we redesignated his affectation status as "unknown."

Subsequently, we genotyped additional STR markers proximal to D5S636, the previously defined proximal boundary of the critical interval. Lack of homozygosity in affected individuals 21, 27, and 29 at marker D5S2090 suggested the causal mutation lies distal to marker D5S2090 extending the critical interval with significant two-point LOD scores (Table 2). The new critical interval included *PDE6A*, a gene previously associated with RP. We sequenced all the coding exons, exon–intron boundaries along with the 5′ and 3′ untranslated regions (UTRs) of *PDE6A* that identified a variation in intron 16 at the splice acceptor site substituting guanine for adenosine at position −1: c.2028–1G>A. The mutation segregated with disease phenotype in the family (Figure 1 and Figure 4A-C) except individual 17 (heterozygous carrier of the c.2028–1G>A variation) and was absent in 350 ethnically matched control chromosomes. This variation was not present in the 1000 Genomes and NHLBI Exome Sequencing Project databases.

We were confident that c.2028–1G>A is responsible for the RP phenotype in PKRP133 provided that (a) two genome scans localized the critical interval chromosome 5q, (b) *PDE6A* has been previously implicated in the pathogenesis of retinal dystrophies including RP, and (c) the splice acceptor site mutations at positions −1 and −2 are considered deleterious. Nonetheless, we sought additional evidence to exclude the possibility that a variant other than c.2028–1G>A present within the critical interval is responsible for the disease phenotype. We captured the entire exome of individual 29 using the SureSelect Human All Exon Kit and sequenced on the Illumina HiSeq 2000 Genome Analyzer (Illumina). We identified 37 additional variants present within the critical interval excluding the splice-acceptor site variant (c.2028–1G>A) identified with Sanger sequencing; however, none of them satisfied the inclusion criterion of causality, which includes (a) absence or a low minor allele frequency in the 1000 Genomes and NHLBI Exome Sequencing Project databases; (b) absence from ethnically matched control chromosomes; and (c) segregation with the disease phenotype in the respective family, further confirming that c.2028–1G>A is responsible for the RP phenotype in PKRP133.

Next, we interrogated our entire cohort of RP familial cases by genotyping STR markers that span the *PDE6A* followed by bidirectional sequencing of the coding exons and exon–intron boundaries. We identified an additional familial case, PKRP140 (Figure 4D), who harbored a splice acceptor site mutation in intron 10: c.1408–2A>G (Figure 4E-G). We recruited a total of 15 individuals of PKRP140; ten of these participating individuals manifested symptoms of RP. The splice acceptor mutation segregated with the disease phenotype (RP) in the family (Figure 4D-G) and was not found in 350 ethnically matched control chromosomes and the 1000 Genomes and NHLBI Exome Sequencing Project databases. We further evaluated the conservation of c.1408–2A and c.2028–1G in other *PDE6A* orthologs. As shown in Figure 5, c.1408–2A and c.2028–1G are fully conserved in primates, placental mammals, and vertebrate *PDE6A* orthologs.

We used HSF, a freely available online bioinformatics tool, to predict the effect of the c.1408–2A and c.2028–1G variations on *PDE6A* mRNA splicing. The HSF analysis

Table 1. Clinical characteristics of members of family PKRP133.

ID	Age (years)	Age at first diagnosis	First symptoms	Night blindness	Fundus examination	ERG		Visual Acuity	
						OD	OS	OD	OS
21	55	Early childhood	NB	Progressive	MD, Art.atten., Pig.dep PD	NAB, NF	NAB, NF	C.F	C.F
30	27	Early childhood	NB	Progressive	MD, Art.atten., Pig.dep PD	NAB, NF	NAB, NF	6/50	6/50
33	24	N/A	Nil	N/A	Normal	Normal	Normal	6/6	6/6
41	27	N/A	Nil	N/A	Normal	Normal	Normal	6/6	6/6

MD, macular degeneration; Art. atten, artery attenuation; Pig.dep, pigment deposit and PD, Pale optic disc. NAB: no 'a' or 'b' wave response; NF: no flicker response; OD and OS as defined in Figure 2.

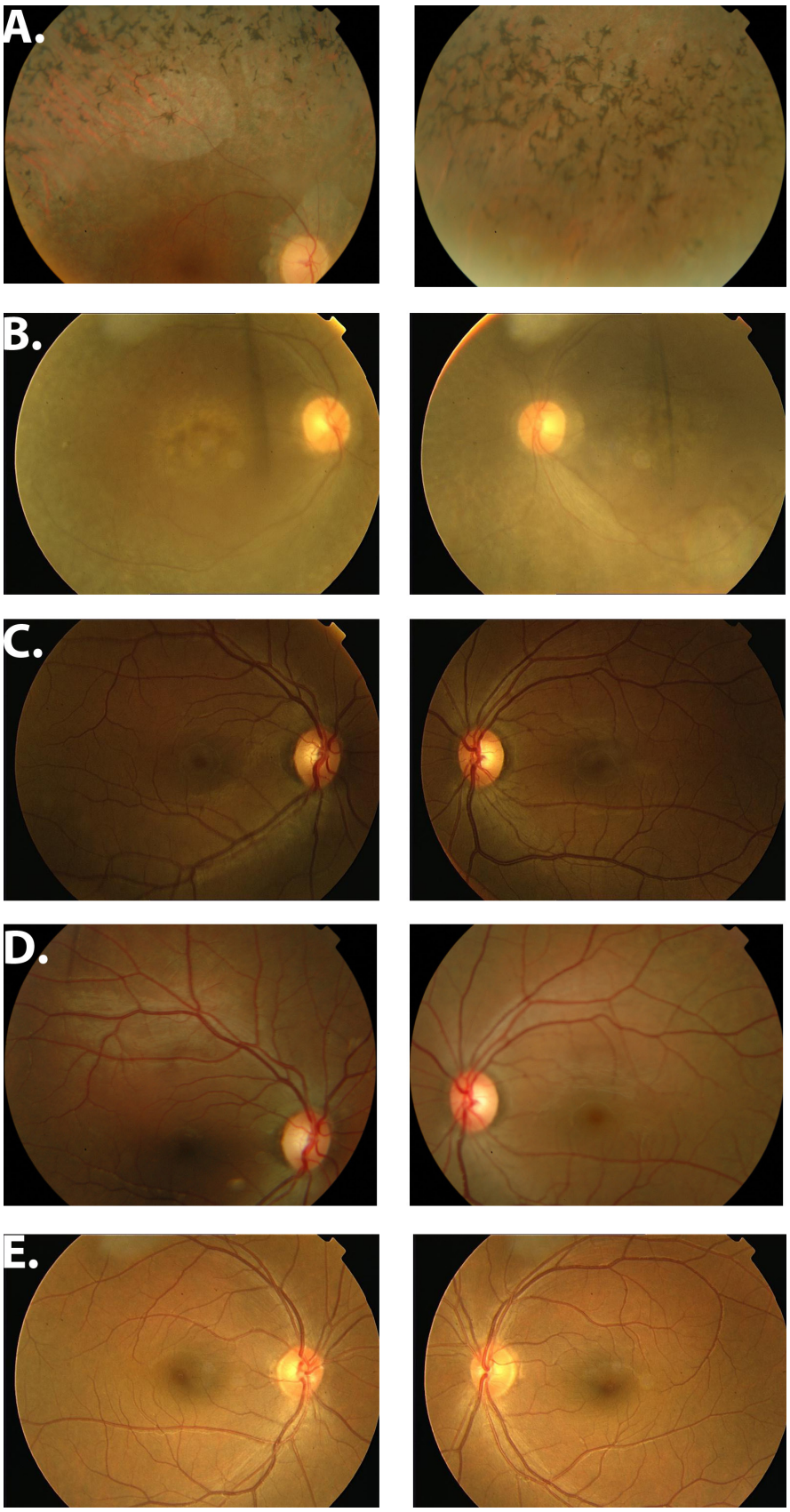

Figure 2. Fundus photographs of family PKRP133. **A**: OD and OS of individual 21. **B**: OD and OS of individual 30. **C**: OD and OS; individual 33 (examined at the age of 22 years). **D**: OD and OS of individual 33 (examined at the age of 24 years). **E**: OD and OS of individual 41. Fundus photographs of the affected individuals show attenuated arteries, bone spicule-like pigmentation, and slightly tilted waxy optic discs. OD=oculus dexter (right eye); OS=oculus sinister (left eye).

generated consensus values of 81.30 and 52.35 for the wild-type (c.1408–2A) and mutant (of c.1408–2G) nucleotides, respectively. The predicted consensus deviation value of −35.61% for c.1408–2A>G suggests the loss of the wild-type splice site that would result in the skipping of exon 11 of PDE6A (Figure 6A). Likewise, HSF analysis predicted the consensus values of 82.23 and 53.28 for the wild-type (c.2028–1G) and mutant (c.2028–1A) nucleotides, respectively. The predicted deviation of −35.21% for c.2028–1G>A suggests the loss of the wild-type splice acceptor site of exon 17 (Figure 6B-C). In parallel, HSF also detected the creation of a new cryptic splice acceptor site using the G nucleotide (c.2028G) in exon 17 (Figure 6D). The algorithm predicted consensus values of 45.37 and 74.31 for the wild-type (c.2028–1G) and the new cryptic splice site (c.2028G), respectively. The predicted consensus value deviation of +63.81% for the new cryptic splice acceptor site suggests the loss of the wild-type splice site that would result in a frame-shift and eventually would lead to a premature stop codon (p.K677Rfs24*) in the protein.

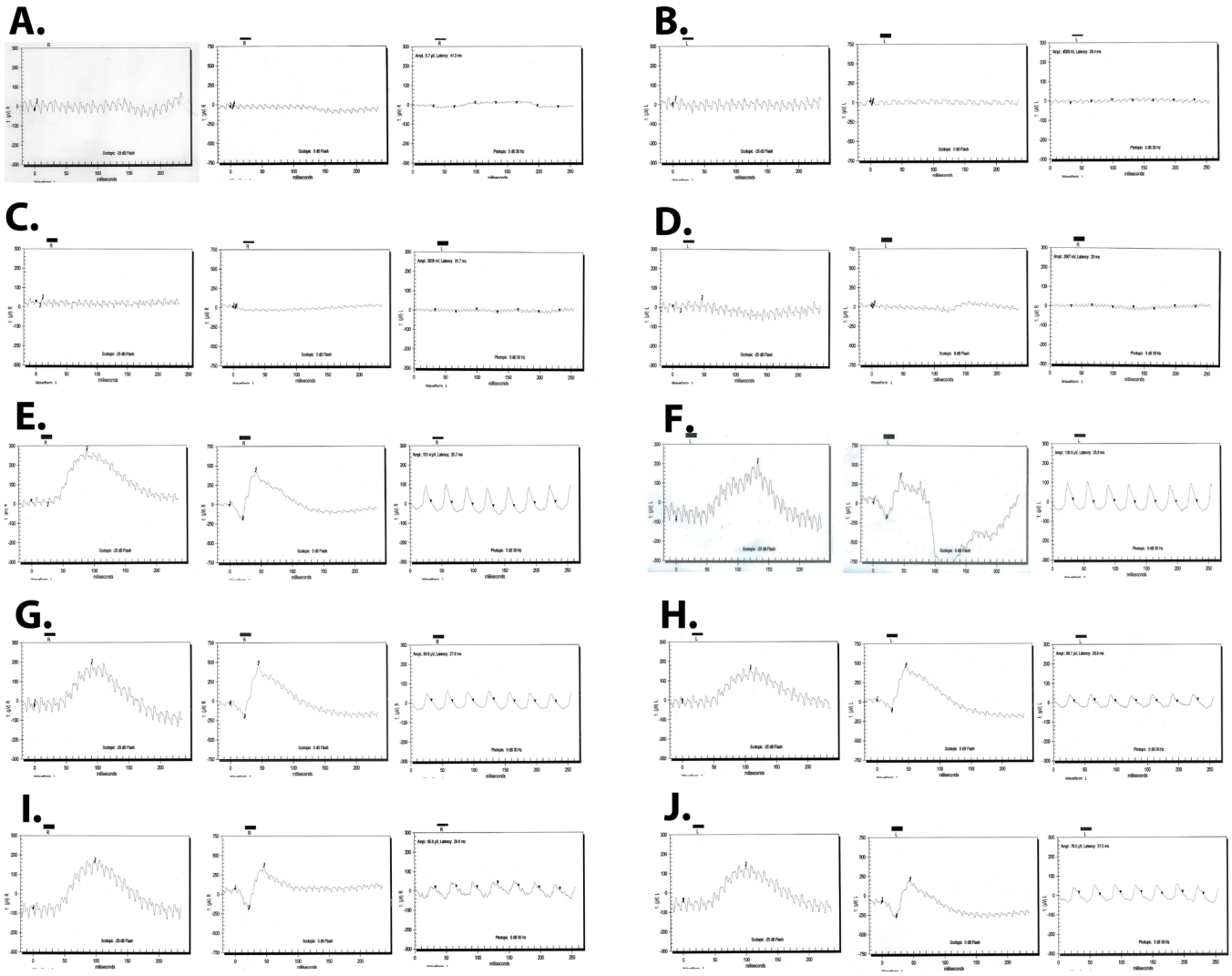

Figure 3. Electroretinography recordings of family PKRP133. Scotopic −25 dB, scotopic 0 dB response, and photopic 0 dB 30Hz flicker response of **A**) OD and **B**) OS of individual 21; **C**) OD and **D**) OS of individual 30; **E**) OD and **F**) OS of individual 33 (examined at the age of 22 years); **G**) OD and **H**) OS of individual 33 (examined at the age of 24 years); **I**) OD and **J**) OS of unaffected individual 41. Affected individuals 21 and 30 manifest typical retinitis pigmentosa (RP) changes on electroretinography (ERG), including loss of the rod and cone responses, while the ERG readings of unaffected individuals 33 and 41 show normal rod and cone responses. OD=oculus dexter (right eye); OS=oculus sinister (left eye).

Table 2. Two-point LOD scores of chromosome 5q markers for family PKRP133.

Marker	cM	Mb	0	0.01	0.05	0.1	0.2	0.3	Z_{max}	θ_{max}
D5S2090	150.34	147.22	−3.32	0.24	0.85	0.98	0.83	0.51	0.98	0.10
D5S636	153.17	149.89	3.17	3.11	2.86	2.52	1.80	1.09	3.17	0.00
D5S2026	157.41	153.86	3.66	3.60	3.35	3.00	2.23	1.39	3.66	0.00
D5S1507	157.57	155.24	- ∞	2.3	2.65	2.5	1.88	1.18	2.65	0.05
D5S2852	158.12	155.42	- ∞	2.32	2.66	2.53	1.89	1.21	2.66	0.05
D5S1971	161.94	158.54	∞	0.66	1.1	1.09	0.77	0.4	1.1	0.05
D5S422*	164.19	162.15	- ∞	2.33	2.67	2.52	1.91	1.18	2.67	0.05
D5S2066	165.13	163.35	2.84	2.77	2.52	2.2	1.54	0.88	2.84	0.00
D5S2050*	171.06	166.51	- ∞	2.28	2.64	2.5	1.87	1.1	2.64	0.05
D5S400*	174.80	168.44	- ∞	1.84	2.24	2.16	1.67	1.06	2.24	0.05
D5S625	177.06	170.17	- ∞	2.11	2.46	2.32	1.75	1.09	2.46	0.05
D5S1960$	179.11	171.51	- ∞	2.6	2.95	2.81	2.19	1.4	2.95	0.05
D5S2069	182.35	173.10	- ∞	1.84	2.32	2.27	1.78	1.1	2.32	0.05
D5S2111	187.81	176.04	- ∞	0.1	1.17	1.35	1.14	0.71	1.35	0.1

Asterisk (*) and dollar ($) symbols indicate the markers included in genome-wide scan using Linkage mapping set v.2.5-HD10 and HD5, respectively. Linkage analysis was performed with alleles of PKRP133 using the FASTLINK version of MLINK while maximum LOD scores were calculated using ILINK from the LINKAGE Program Package.

DISCUSSION

We report in this study two splicing acceptor site mutations in *PDE6A* associated with autosomal recessive RP in two large consanguineous Pakistani families. Two-point LOD scores of 3.66 and 3.17 for markers D5S2026 and D5S636, respectively, the absence of any scores >1.5 observed during genome-wide linkage scan other than on 5q, identification of variations in evolutionary conserved bases, c.1408–2A and c.2028–1G, and the absence of these variations in ethnically matched control chromosomes, 1000 Genomes and NHLBI Exome Sequencing Project databases strongly support our conclusion that the two splice acceptor site mutations are responsible for the retinal phenotype of the patients reported in this study.

In silico analysis predicted that a splice-site mutation (c.1408–2A>G) would destroy the splice acceptor site, which would result in the skipping of exon 11. Exon 11 consists of 66 base pairs, and thus, skipping of exon 11 would introduce the deletion of 22 amino acids (p.K470_L491del) without disturbing the reading frame of PDE6A. The simple modular architecture research tool (SMART) identified two cGMP-specific phosphodiesterases, adenylyl cyclases and FhlA (GAF) domains (73–232 and 254–441 amino acids), two low-complexity regions (478–495 and 823–851 amino acids), and one PDEase catalytic domain (3′5′-cyclic nucleotide phosphodiesterase) ranging from 556 to 734 amino acids. Based on the PDE6A protein domain structure, this deletion will eliminate the low-complexity region (478–495 amino acids).

However, two possible scenarios are predicted for the splice site c.2028–1G>A mutation: (a) the creation of a new cryptic splice acceptor site using the first G nucleotide of exon 17 and (b) the less likely scenario of the complete skipping of exon 17. The inclusion of this cryptic acceptor site would lead to a frameshift and would ultimately result in a premature termination: p.K677Rfs24* (Figure 6D). The mutant mRNA would be degraded by the nonsense mediated decay (NMD) pathway. Even if the protein escapes the NMD pathway, the truncated protein would lack 160 C-terminal amino acids including the cGMP-binding site and one low-complexity region. However, skipping exon 17, which comprises 108 bp, would result in a deletion composed of 36 amino acids (p.K676_M712del) without altering the reading frame of PDE6A but would disrupt the PDEase catalytic domain (Figure 6D).

To date, 20 causal mutations in *PDE6A* have been associated with RP including ten missense, five nonsense, two splice site, two frameshift, and a deletion encompassing the entire gene [14,15,20–26]. Dryja and colleagues screened sporadic and recessive RP cases and found that mutations in *PDE6A* are responsible for the clinical phenotype in 3% of Caucasian patients [21]. Previously, our group identified mutations in *PDE6A* in three consanguineous families [15]. Taking these results together, we have identified five families in our cohort of >300 familial cases suggesting an approximate 2% contribution to the total genetic load of RP.

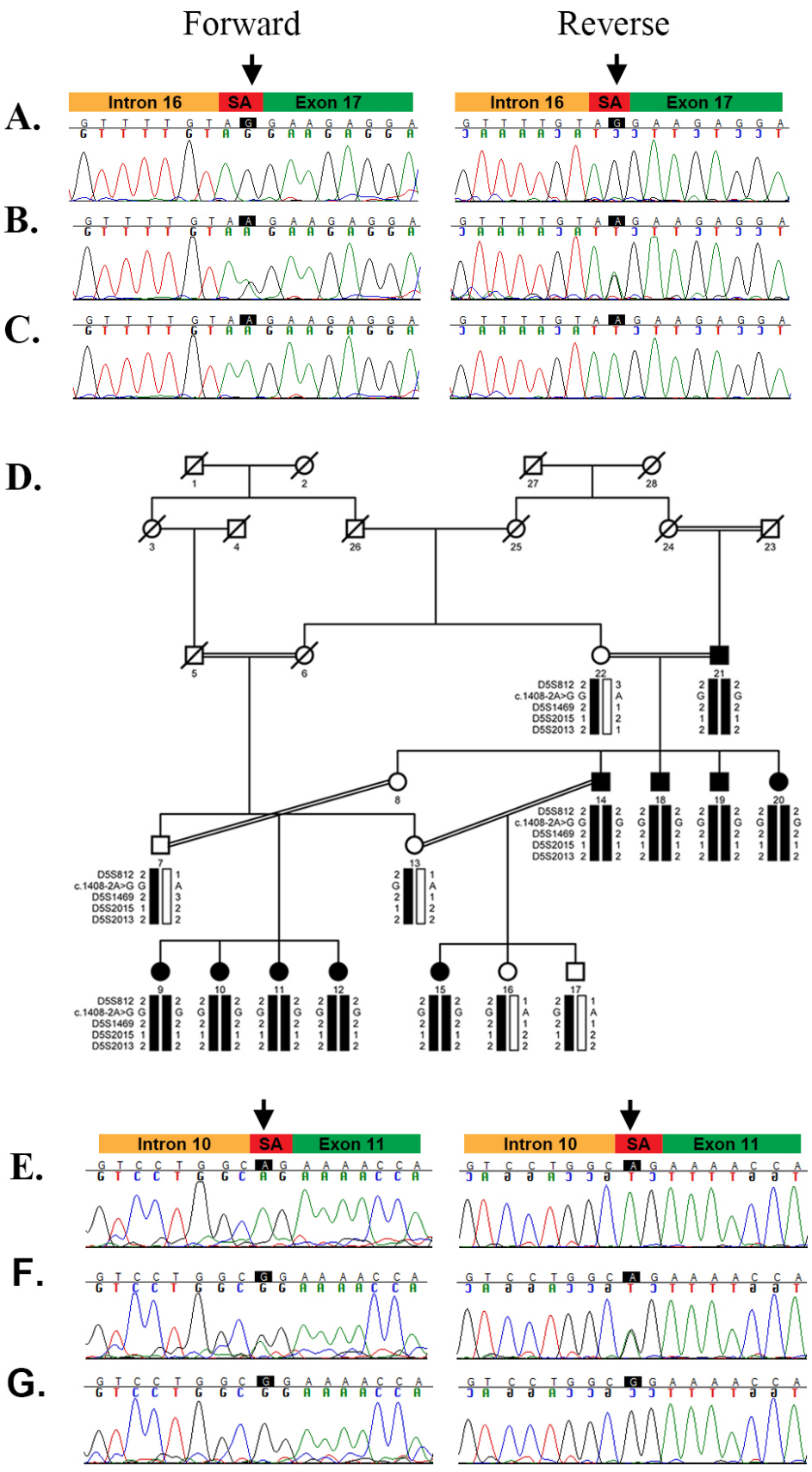

Figure 4. Causal variants in *PDE6A* identified in families PKRP133 and PKRP140. **A**: Sequence chromatogram of unaffected individual 15 homozygous for the wild-type. **B**: Sequence chromatogram of unaffected individual 28 heterozygous carriers. **C**: Sequence chromatogram of affected individual 29 of PKRP133 homozygous for the G to A variation in intron 16; c.2028–1G>A. **D**: Pedigree of family PKRP140 with the haplotypes of four adjacent chromosome 5q33 microsatellite markers are shown with the alleles forming the risk haplotype shaded black and the wild-type allele shown in white. Squares are males, circles are females, filled symbols are affected individuals, the double line between individuals indicates consanguinity, and the diagonal line through a symbol is a deceased family member. **E**: Sequence chromatogram of unaffected control homozygous for the wild-type. **F**: Sequence chromatogram of individual 13 heterozygous carrier. **G**: Sequence chromatogram of affected individual 14 of PKRP140 homozygous for the A to G transition in intron 10: c.1408–2A>G. The arrows point to the splice site variation identified in families PKRP133 (c.2028–1G) and PRKP140 (c.1408–2A) whereas green, red, and brown represent the exon, splice acceptor site, and intron, respectively. SA=splice acceptor.

Human	c.1408A	c.1408-1G	c.1408 -2A	c.1408-3C	c.1408-4G	c.2027A	c.2028G	c.2028-1G	c.2028-2A	c.2028-3T
Chimp	A	G	A	C	G	A	G	G	A	T
Gorrila	A	G	A	C	G	A	G	G	A	T
Orangutan	A	G	A	C	G	A	G	G	A	T
Gibbon	A	G	A	C	G	A	G	G	A	T
Rhesus	A	G	A	C	G	A	G	G	A	T
Crab-eating macaque	A	G	A	C	G	A	G	G	A	T
Baboon	A	G	A	C	G	A	G	G	A	T
Green monkey	A	G	A	C	G	A	G	G	A	T
Marmoset	A	G	A	C	G	A	G	G	A	T
Squirrel monkey	A	G	A	C	G	A	G	G	A	T
Bushbaby	A	G	A	C	G	A	G	G	A	T
Chinese tree shrew	A	G	A	C	G	A	G	G	A	T
Squirrel	A	G	A	C	G	A	G	G	A	T
Lesser Egyptian jerboa	A	G	A	C	G	A	G	G	A	T
Praire vole	A	G	A	C	G	A	G	G	A	C
Chinese hamster	A	G	A	C	G	A	G	G	A	C
Golden hamster	A	G	A	A	G	A	G	G	A	C
Mouse	A	G	A	C	-	-	-	-	-	-
Rat	A	G	A	C	G	A	G	G	A	C
Naked mole rat	A	G	A	C	G	A	G	G	A	T
Guniea pig	A	G	A	C	G	A	G	G	A	T
Chinchilla	A	G	A	C	G	A	G	G	A	T
Brush tailed rat	A	G	A	C	G	A	G	G	A	T
Rabbit	A	G	A	C	G	A	G	G	A	T
Pika	A	G	A	C	G	A	G	G	A	T
Pig	A	G	A	C	G	A	G	G	A	C
Alpaca	A	G	A	C	G	A	G	G	A	T
Bactrian camel	A	G	A	C	G	A	G	G	A	T
Dolphin	A	G	A	C	G	A	G	G	A	T
Killer whale	A	G	A	C	G	A	G	G	A	T
Tibetan antelope	A	G	A	T	G	A	G	G	A	T
Sheep	A	G	A	C	G	A	G	G	A	T
Domestic goat	A	G	A	C	G	A	G	G	A	T
Horse	A	G	A	C	G	A	G	G	A	T
White rhinoceros	A	G	A	C	G	A	G	G	A	T
Cat	A	G	A	C	G	A	G	G	A	C
Dog	A	G	A	C	G	A	G	G	A	C
Ferret	A	G	A	C	G	A	G	G	A	C
Panda	A	G	A	C	G	A	G	G	A	C
Pacific walrus	A	G	A	C	G	A	G	G	A	C
Weddell seal	A	G	A	C	G	A	G	G	A	C
Black flying fox	A	G	A	T	G	A	G	G	A	T
Megabat	A	G	A	T	G	A	G	G	A	T
David's myotis (bat)	A	G	A	-	-	A	G	G	A	T
Microbat	A	G	A	-	-	A	G	G	A	T
Big brown bat	A	G	A	-	-	A	G	G	A	T
Hedgehog	A	G	A	C	G	A	G	G	A	T
Shrew	A	G	A	C	G	A	G	G	A	T
Star nosed mole	A	G	A	C	G	A	G	G	A	T
Elephant	A	G	A	C	G	A	G	G	A	T
Cape elephant shrew	A	G	A	T	G	A	G	G	A	T
Manatee	A	G	A	C	G	A	G	G	A	T
Cape golden mole	A	G	A	C	G	A	G	G	A	T
Tenrec	A	G	A	C	G	A	G	G	A	T
Aardvark	A	G	A	C	G	A	G	G	A	C
Armadillo	A	G	A	C	G	A	G	G	A	T
Opossum	A	G	A	C	C	A	G	G	A	C
Tasmanian devil	A	G	A	C	T	A	A	G	A	C
Wallaby	A	G	A	C	T	A	A	G	A	C
Platypus	A	G	A	C	-	A	A	G	A	C

Figure 5. Sequence alignment illustrating the conservations of *PDE6A* splice acceptor sites. c.2028–1G and c.1408–2A are fully conserved in the *PDE6A* orthologs. The organisms in brown and blue are primates and placental mammals, respectively, and the c.2028–1G and c.1408–2A variations are in red.

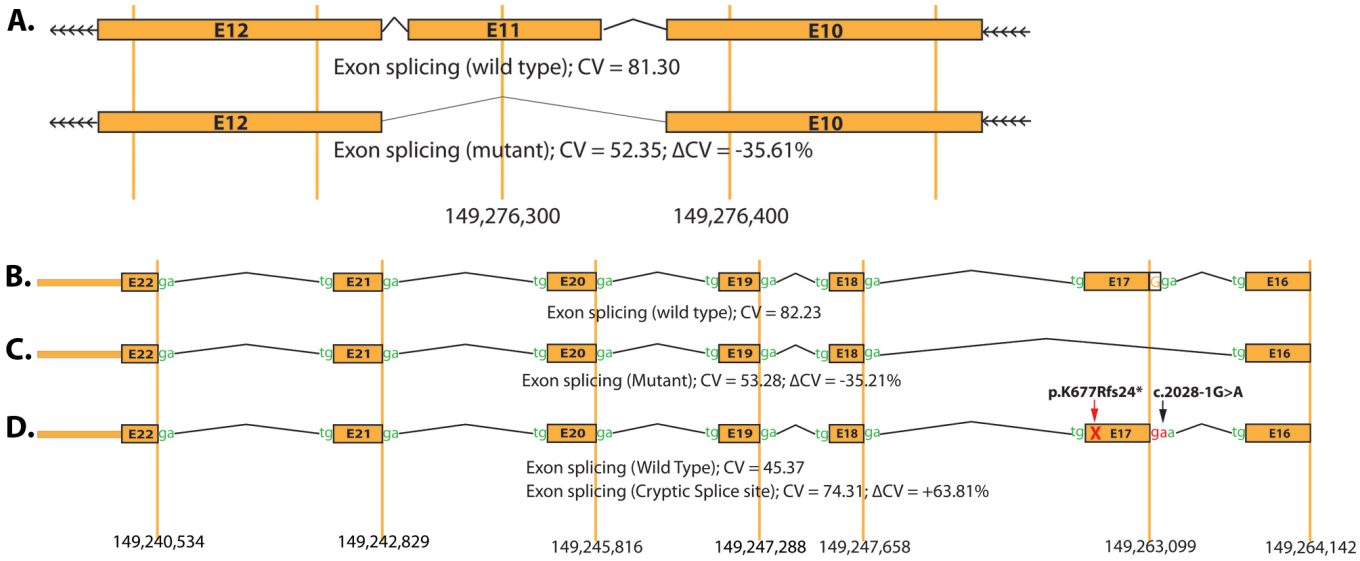

Figure 6. Predictive outcome of *PDE6A* splice acceptor site variations on the exon splicing mechanism. **A**: Ideograms illustrate the skipping of exon 11 due to a splice acceptor site mutation at position −2 of intron 10: c.1408–2A>G. **B**–**D**: Ideograms illustrate the predictive splicing patterns of exon 17 due to the splice acceptor site mutation at position −1 of intron 16: c.2028–1G>A. **B**: The prediction of a strong consensus value (CV) of 82.23 for the wild-type splice acceptor site (c.2028–1G). **C**: A possible scenario that would result in the skipping of exon 17 during mRNA processing. **D**: Predicting the creation of a new cryptic splice acceptor site (CV=74.31) with predicted deviation (ΔCV) of +63.81% that would result in the premature stop codon (p.K677Rfs24*) and eventually would lead to a truncated protein. CV=consensus values; ΔCV=reduction in consensus values.

In conclusion, we identified two splice acceptor site mutations segregated in two large consanguineous pedigrees responsible for arRP. The identification of causal mutations will enhance diagnostic capabilities leading to the identification of carrier status, which would help in the prevention of the familial form of arRP.

ACKNOWLEDGMENTS

We are thankful to all family members for their participation in this study. This study was supported in part by Higher Education Commission (HEC), Islamabad Pakistan and Ministry of Science and Technology, Islamabad, Pakistan, and by the National Eye Institute Grant R01EY021237–01 (RA and SAR).

REFERENCES

1. Donders F. Beiträge zur pathologischen Anatomie des Auges. 2. Pigmentbildung in der Netzhaut. Arch Ophthalmol 1857; 3:139-65. .
2. Bird AC. Retinal photoreceptor dystrophies LI. Edward Jackson Memorial Lecture. Am J Ophthalmol 1995; 119:543-62. [PMID: 7733180].
3. Weleber RGaG-EK. *Retinitis pigmentosa and allied disorders*. Ryan, S.J. (ed.), ed.; 2001:362–470.
4. Rivolta C, Sharon D, DeAngelis MM, Dryja TP. Retinitis pigmentosa and allied diseases: numerous diseases, genes, and inheritance patterns. Hum Mol Genet 2002; 11:1219-27. [PMID: 12015282].
5. Nadeau JH. Modifier genes in mice and humans. Nat Rev Genet 2001; 2:165-74. [PMID: 11256068].
6. Grünfeld JP. Monogenic renal diseases: a clinical introduction. J Nephrol 2002; 15:Suppl 6S43-6. [PMID: 12515373].
7. Summers KM. Relationship between genotype and phenotype in monogenic diseases: relevance to polygenic diseases. Hum Mutat 1996; 7:283-93. [PMID: 8723677].
8. Kaupp UB, Niidome T, Tanabe T, Terada S, Bönigk W, Stühmer W, Cook NJ, Kangawa K, Matsuo H, Hirose T, Miyata T, Numa S. Primary structure and functional expression from complementary DNA of the rod photoreceptor cyclic GMP-gated channel. Nature 1989; 342:762-6. [PMID: 2481236].
9. Chen TY, Peng YW, Dhallan RS, Ahamed B, Reed RR, Yau KW. A new subunit of the cyclic nucleotide-gated cation channel in retinal rods. Nature 1993; 362:764-7. [PMID: 7682292].
10. Stryer L. The molecules of visual excitation. Sci Am 1987; 257:42-50. [PMID: 3037690].
11. Taylor RE, Shows KH, Zhao Y, Pittler SJA. PDE6A promoter fragment directs transcription predominantly in the photoreceptor. Biochem Biophys Res Commun 2001; 282:543-7. [PMID: 11401494].

12. Pittler SJ, Baehr W, Wasmuth JJ, McConnell DG, Champagne MS, vanTuinen P, Ledbetter D, Davis RL. Molecular characterization of human and bovine rod photoreceptor cGMP phosphodiesterase alpha-subunit and chromosomal localization of the human gene. Genomics 1990; 6:272-83. [PMID: 2155175].

13. Mohamed MK, Taylor RE, Feinstein DS, Huang X, Pittler SJ. Structure and upstream region characterization of the human gene encoding rod photoreceptor cGMP phosphodiesterase alpha-subunit. J Mol Neurosci 1998; 10:235-50. [PMID: 9770645].

14. Dryja TP, Finn JT, Peng YW, McGee TL, Berson EL, Yau KW. Mutations in the gene encoding the alpha subunit of the rod cGMP-gated channel in autosomal recessive retinitis pigmentosa. Proc Natl Acad Sci USA 1995; 92:10177-81. [PMID: 7479749].

15. Riazuddin SA, Zulfiqar F, Zhang Q, Yao W, Li S, Jiao X, Shahzadi A, Amer M, Iqbal M, Hussnain T, Sieving PA, Riazuddin S, Hejtmancik JF. Mutations in the gene encoding the alpha-subunit of rod phosphodiesterase in consanguineous Pakistani families. Mol Vis 2006; 12:1283-91. [PMID: 17110911].

16. Miller SA, Dykes DD, Polesky HF. A simple salting out procedure for extracting DNA from human nucleated cells. Nucleic Acids Res 1988; 16:1215-[PMID: 3344216].

17. Grimberg J, Nawoschik S, Belluscio L, McKee R, Turck A, Eisenberg A. A simple and efficient non-organic procedure for the isolation of genomic DNA from blood. Nucleic Acids Res 1989; 17:8390-[PMID: 2813076].

18. Lathrop GM, Lalouel JM. Easy calculations of lod scores and genetic risks on small computers. Am J Hum Genet 1984; 36:460-5. [PMID: 6585139].

19. Schäffer AA, Gupta SK, Shriram K, Cottingham RW Jr. Avoiding recomputation in linkage analysis. Hum Hered 1994; 44:225-37. [PMID: 8056435].

20. Huang SH, Pittler SJ, Huang X, Oliveira L, Berson EL, Dryja TP. Autosomal recessive retinitis pigmentosa caused by mutations in the alpha subunit of rod cGMP phosphodiesterase. Nat Genet 1995; 11:468-71. [PMID: 7493036].

21. Dryja TP, Rucinski DE, Chen SH, Berson EL. Frequency of mutations in the gene encoding the alpha subunit of rod cGMP-phosphodiesterase in autosomal recessive retinitis pigmentosa. Invest Ophthalmol Vis Sci 1999; 40:1859-65. [PMID: 10393062].

22. Poehner WJ, Fossarello M, Rapoport AL, Aleman TS, Cideciyan AV, Jacobson SG, Wright AF, Danciger M, Farber DB. A homozygous deletion in RPE65 in a small Sardinian family with autosomal recessive retinal dystrophy. Mol Vis 2000; 6:192-8. [PMID: 11062306].

23. Tsang SH, Tsui I, Chou CL, Zernant J, Haamer E, Iranmanesh R, Tosi J, Allikmets R. A novel mutation and phenotypes in phosphodiesterase 6 deficiency. Am J Ophthalmol 2008; 146:780-8. [PMID: 18723146].

24. Corton M, Blanco MJ, Torres M, Sanchez-Salorio M, Carracedo A, Brion M. Identification of a novel mutation in the human PDE6A gene in autosomal recessive retinitis pigmentosa: homology with the nmf28/nmf28 mice model. Clin Genet 2010; 78:495-8. [PMID: 21039428].

25. Corton M, Nishiguchi KM, Avila-Fernández A, Nikopoulos K, Riveiro-Alvarez R, Tatu SD, Ayuso C, Rivolta C. Exome sequencing of index patients with retinal dystrophies as a tool for molecular diagnosis. PLoS ONE 2013; 8:e65574-[PMID: 23940504].

26. Saqib MA, Nikopoulos K, Ullah E, Sher Khan F, Iqbal J, Bibi R, Jarral A, Sajid S, Nishiguchi KM, Venturini G, Ansar M, Rivolta C. Homozygosity mapping reveals novel and known mutations in Pakistani families with inherited retinal dystrophies. Sci Rep 2015; 5:9965-[PMID: 25943428].

Articles are provided courtesy of Emory University and the Zhongshan Ophthalmic Center, Sun Yat-sen University, P.R. China. The print version of this article was created on 18 August 2015. This reflects all typographical corrections and errata to the article through that date. Details of any changes may be found in the online version of the article.